Development of High Ductility and Tensile Properties upon Two-Stage Draw of Ultrahigh Molecular Weight Poly(acrylonitrile)

Akira Yamane, Daisuke Sawai, Tsunenori Kameda, and Tetsuo Kanamoto*

Department of Applied Chemistry, Science University of Tokyo, Kagurazaka, Shinjuku-ku, Tokyo 162, Japan

Masayoshi Ito

Department of Chemistry, Science University of Tokyo, Kagurazaka, Shinjuku-ku, Tokyo 162, Japan

Roger S. Porter

Polymer Science & Engineering, University of Massachusetts, Amherst, Massachusetts 01003

Received September 23, 1996; Revised Manuscript Received January 22, 1997[⊗]

ABSTRACT: Solutions (1−5 wt %) of ultrahigh-molecular-weight atactic poly(acrylonitrile) (UHMW-PAN) in *N*,*N*′-dimethylformamide were crystallized to gel by quenching from 100 to 0 °C. The dried gel films exhibited poor ductility on straight tensile draw. However, they were ductile on solid-state coextrusion to an extrusion draw ratio (EDR) of 8−16 (first-stage draw). Thus, the initially coextrusion drawn films were further drawn by a tensile force (second-stage draw). Drawability of the gel film was strongly influenced by several factors, including the solution concentration from which gel was made, first-stage EDR, and second-stage draw temperature. With increasing prior solution concentration, the ductility of a gel film decreased. The maximum achieved total draw ratio ($DR_{t,max}$) by the two-stage draw and the uniformity of drawn products increased with first-stage EDR. Further, the ductility increased rapidly above ∼150 °C, reaching a maximum at ∼190 °C, and decreased at yet higher temperatures. A $DR_{t,max}$ of ∼110 was achieved under optimum conditions. The efficiency of draw was lower for a gel film prepared from a lower solution concentration, as evaluated by the crystalline orientation function (f_c) and tensile properties vs DR. The highest f_c of 0.998, and tensile modulus of 26 GPa and strength of 1.3 GPa were obtained by ultradrawing of the gel films, with a prior solution concentration of 1−2 wt %. Further, the modulus is close to the uncertain X-ray crystal modulus of atactic PAN (28 GPa). The wide-angle X-ray diffraction patterns measured at room temperature showed an orthorhombic chain packing with significant disorder along the chain axis, independent of draw temperature and DR. Further, the temperature variations of the orthorhombic $(200)_o$ and $(110)_o$ spacings revealed that the initially orthorhombic cell transforms to the hexagonal unit cell around 150 °C. Thus, the rapid increase in ductility above ∼150 °C is ascribed to the existence of this reversible crystal/crystal transition, above which the molecular motion in crystalline regions is activated.

Introduction

Polymers with strong intermolecular interactions and/or a rigid chain generally exhibit only low ductility, independent of variables including chain entanglement density, sample molecular weight, and draw temperature. Illustrations are the low ductility of nylons[1−3] and poly(ethylene telephthalate).[4,5] The maximum achieved draw ratios and tensile moduli for these two polymers were in the range of 10−15 and 15−30% for each of their crystal moduli, respectively.

Poly(acrylonitrile) (PAN) is a polymer of high cohesive energy density and fairly high chain stiffness,[6] due to the bulky nitrile groups with a large dipole. This polymer, thus, has a high estimated melting temperature (T_m) of 317 °C[7] and undergoes thermal degradation below the T_m. Further, the crystallinity and its change on draw are difficult to determine, because the amorphous density is not known. In spite of such characteristics, it was shown that ultrahigh-molecular-weight atactic poly(acrylonitrile) (UHMW-PAN) gel films[8] and common molecular weight nascent PAN powder films[9] can be ultradrawn by solid-state coextrusion to an extrusion draw ratio (EDR) of 70−85 at the optimum extrusion temperature range of 140−160 °C. The PAN powder film was obtained by filtering the suspension of lamellar crystals precipitated during thermal polymerization of acrylonitrile (AN).[10] The maximum achieved tensile modulus and strength were 20 and 1.0 GPa, respectively, for the UHMW-PAN[8] and 13 and 0.4 GPa, respectively, for the common molecular weight nascent PAN.[9] The highest modulus achieved corresponds to 70% of the uncertain X-ray crystal modulus of atactic PAN (28 GPa[11]) but is significantly lower than the highest reported modulus of 30 GPa[12] for an UHMW-PAN fiber.

A two-stage drawing technique has successfully been applied for ultradrawing of various polymers, including single crystal mats of UHMW-polyethylene,[13] UHMW-polypropylene,[14] and UHMW-poly(4-methyl-1-pentene)[15] and reactor powders of UHMW-polyethylene,[16] poly(tetrafluoroethylene),[17] and common molecular weight PAN.[9] Among these, single crystal mats of the first three have been superdrawn to the limit in terms of tensile modulus approaching the X-ray crystal modulus for each of these polymers. Such high ductility of single crystal mats has been ascribed to their low entangled state.

[⊗] Abstract published in *Advance ACS Abstracts,* June 15, 1997.

S0024-9297(96)01409-X CCC: $14.00

As reported in this paper, dried gel films of UHMW-PAN were drawn by the two-stage drawing technique,[13] which consists of the first-stage solid-state coextrusion[18] followed by the second-stage tensile draw at controlled temperatures and rates. The effects of chain entanglement on drawing of gel films and the resultant structure and properties of drawn products have been studied. Further, the high ductility of UHMW-PAN is discussed in relation to the reversible crystal/crystal transition observed by wide-angle X-ray diffraction (WAXD).

Experimental Section

Polymerization. The UHMW-PAN used was prepared by suspension polymerization of AN.[19] A 40 wt % AN aqueous solution was added with 0.1 wt % of AIBN as an initiator and 1.5 wt % of poly(vinyl alcohol) (Kuraray Co. Ltd., LOT-343401) having degrees of polymerization of 2000 and a saponification of 88% as a dispensing agent, both based on the weight of AN. The solution was kept at 60 °C for 1.5 h with high-speed stirring.

The intrinsic viscosity of PAN was measured in dimethyl sulfoxide at 50 °C. The viscosity average molecular weight was calculated to be 1.3×10^6, according to an intrinsic viscosity/molecular weight relation.[20]

Gel Films. Polymer solutions with concentrations ranging from 1 to 5 wt % were prepared by dissolving the requisite amounts of UHMW-PAN in *N*,*N*′-dimethylformaide at 100 °C. The solutions were transferred into stainless trays and quenched at 0 °C for 2 h to make gels. The wet gel films were extracted with methanol and then dried at room temperature in vacuo to constant weight.

Two-Stage Drawing. The dry gel films of UHMW-PAN showed low ductility on straight tensile draw. However, the gel films were ductile on solid-state coextrusion. The initially extrusion drawn films were further drawn by a tensile force to achieve higher draw. For the first-stage coextrusion, a gel film 0.15 mm thick, 5 mm wide, and 60 mm long was placed between two split billet halves of high-density polyethylene, and the assembly was coextruded at 125 °C through conical brass dies with nominal extrusion draw ratios (EDR) of 8−16. EDR was determined from the separation of the ink mark preimprinted on the surface of a gel film. The initially extrusion-drawn films were further drawn by a tensile force at 100−230 °C in an air oven equipped with an Orientec Tensilon tensile tester HTM-100 at constant cross-head speeds (second-stage draw). The draw ratio (DR) for the second-stage draw was also determined by the deformation of ink mark. The total draw ratio (DR_t) was defined by DR_t = (first-stage EDR × second-stage DR).

Characterization. WAXD patterns were recorded by a flat plate camera and by diffractometer scans. Photographs were obtained with Ni-filtered Cu Kα radiation generated at 40 kV and 25 mA on a Rigaku Gigerflex RAD-3A. Diffraction profiles were recorded with Ni-filtered Cu Kα radiation on the same diffractometer equipped with a pulse height discriminator. A high resolution was necessary to detail the crystal structure. The intensity was collected by step scans at 0.02° intervals in 2θ. The reflection profiles were measured by both a symmetrical transmission mode and a symmetrical reflection mode. For the former measurements, line collimators of 0.05 mm (first), 0.15 mm (second), and 0.15 mm (third) were used. For the latter, line collimators of 1/6° (DS), 0.15 mm (RS), and 1/6° (SS) were used. The observed profiles were corrected for the broadening due to instrumental conditions and $K\alpha_1$ and $K\alpha_2$ radiations by using the Rachinger method[21] and Jones curve fitting method.[21] The standard materials used for these corrections were the NBS standard silicon powder and a pure aluminum plate for the reflection and transmission modes, respectively. The apparent crystallite size D_{hkl} perpendicular to the (*hkl*) plane was calculated from the breath at half height, using Sherrer's equation.[21]

Crystalline chain orientation was evaluated by the Herman orientation function, f_c.[21] The azimuthal intensity distribution was recorded by step scans at 0.1° intervals in azimuthal angle, using a Rigaku fiber specimen holder with a first collimator of ϕ = 0.5 mm and a receiving slit of 1.8° (2θ direction) × 0.3° (azimuthal direction).

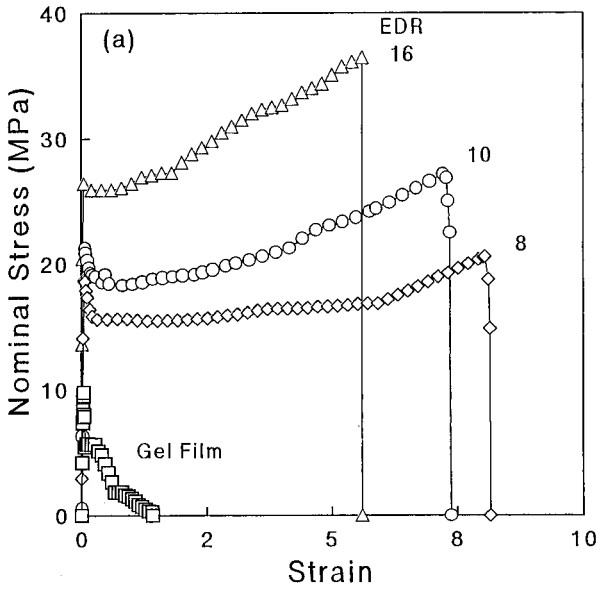

Figure 1. Nominal stress/strain curves for the second-stage draw of a 1 wt % UHMW-PAN gel film and a series of extrusion drawn gel films, recorded at 190 °C.

Densities of drawn products were measured at 30 ± 0.1 °C in a density gradient column consisting of mixtures of *n*-heptane and carbon tetrachloride.

Scanning electron microscopic (SEM) observations of sample surfaces were made on a Hitachi S-5000 scanning electron microscope. Optical microscopic (OM) observations were also made on an Olympus optical microscope, Model BHSP.

The tensile modulus and strength on the film axis were measured at strain rates of 1×10^{-3} and 1×10^{-2}, respectively, at room temperature. The measurements were made at least three times for a given sample. The modulus was determined from the initial slope of the stress/strain curve at low strain (<0.1%). The cross-sectional area of a sample was calculated from the sample weight, length, and measured density.

Results and Discussion

Drawing Behavior. Gel films and initially extrusion-drawn samples, with different EDR's of 8−16, were drawn by a tensile force at various temperatures (T_d). Figure 1 shows nominal stress/strain curves for the second-stage tensile draw of 1 wt % gel films, initially extrusion drawn to different EDRs, tested at 190 °C at a constant cross-head speed corresponding to an initial strain rate of 2/min. The draw stress increased with starting EDR. The maximum achieved DR_t ($DR_{t,max}$) also increased with starting EDR; $DR_{t,max}$ = 2.5, 74, 83, and 110 for starting EDR = 1, 8, 10, and 16, respectively. Such a remarkable increase in drawability of a gel film for the two-stage draw is due to the morphological change that occurred during the first-stage solid-state coextrusion. The as-cast, dried gel film, prepared from a dilute solution of 1−2 wt %, has a few entanglements which may transmit the draw stress. Such a low entangled gel film cannot bear the draw stress for straight tensile drawing and fails at a small strain, as shown in Figure 1. However, during the first-stage solid-state coextrusion to an EDR of 8−16, the gel film consisting of randomly oriented chains transforms into a well-oriented fibrillar structure, which shows an improved strength along the fiber axis. Thus, the gel film prepared from a dilute solution exhibits remarkably higher drawability after having been coextruded to an EDR ≥ 8.

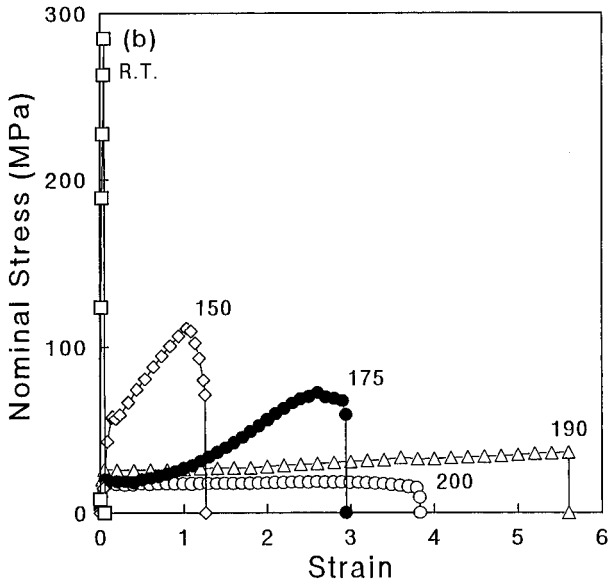

Figure 2. Nominal stress/strain curves for the second stage draw of an EDR 16 extrudate prepared at 125 °C, recorded at different T_d in the range of room temperature to 200 °C. The numbers indicate the second-stage draw temperature, T_d (°C).

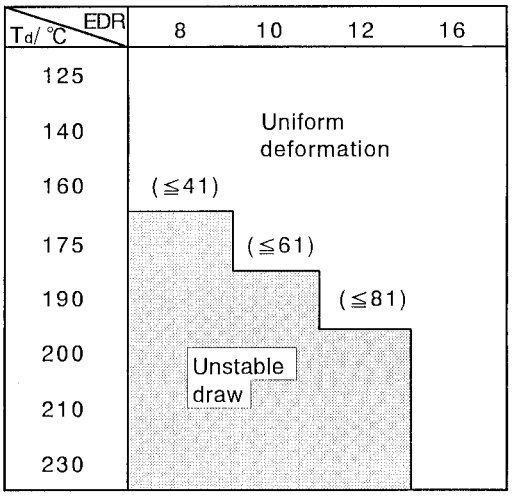

Figure 3. Effects of initial EDR and second-stage T_d on the uniformity of the resultant drawn products and the maximum achieved DR_t. The numbers in the figure represent the maximum achieved DR_t.

Figure 2 shows nominal stress/strain curves for the second-stage draw of an initial EDR 16 extrudate prepared at 125 °C, recorded in the T_d range from room temperature to 200 °C. The draw stress significantly decreased with increasing T_d. No strain hardening occurred for drawing at 190 and 200 °C, as observed on superdrawing of single crystal mats of UHMW-polyethylene[13] and -polypropylene.[14]

Not only the second-stage drawability but also the uniformity of the resultant drawn products were found to be sensitive to the initial EDR and T_d. Figure 3 shows the effects of initial EDR, prepared at 125 °C, and T_d on the deformation characteristics for the second-stage tensile draw of a 1 wt % gel film. Draw was made at constant cross-head speeds corresponding to an initial strain rate of 2/min. On an attempt to draw the gel film directly by tensile draw, a neck developed in the weakest region, and further draw led to fracture. When an extrudate of a low EDR ≤ 12 was tensile-drawn, draw became unstable above a specific temperature, depending on the initial EDR. For an EDR ≥ 16, uniform deformation proceeded in the whole range of T_d studied (≤230 °C). Thus, the extrudates with an EDR of 16 were chosen as starting samples for further second-stage tensile draw.

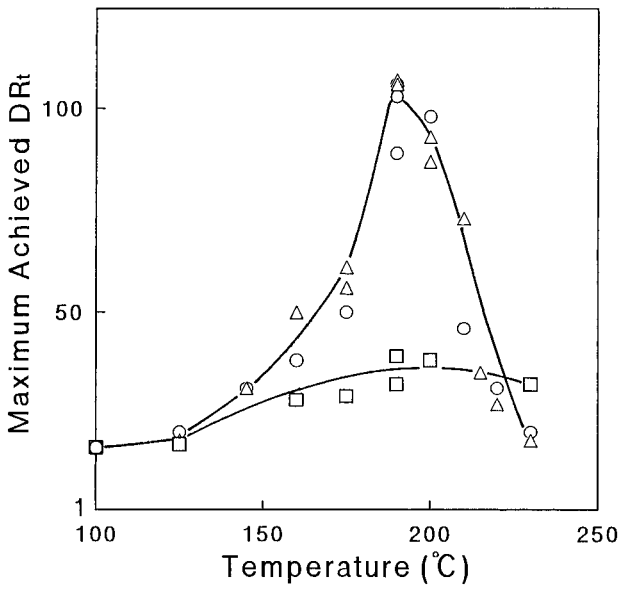

Figure 4. Maximum achieved DR_t as a function of T_d for the second stage tensile drawing of UHMW-PAN gel films prepared from different solution concentrations: ○, gel prepared from 1 wt % solution; △, from 2 wt %; □, from 5 wt %.

Figure 4 shows $DR_{t,max}$ as a function of T_d for the second-stage tensile draw of gel films, prepared from 1−5 wt % solutions and initially extrusion drawn to an EDR of 16. The effect of T_d on ductility is more prominent for the gels prepared from lower solution concentrations, which likely have a lower entanglement density. The $DR_{t,max}$ of gels prepared from 1 and 2 wt % solutions increased markedly with T_d above ∼150 °C, reaching a maximum of 100−110 at an optimum T_d of 190 °C, and decreased sharply at yet higher T_d. In contrast, the drawability of gel, prepared from a higher solution concentration of 5 wt %, was less sensitive to T_d. The maximum DR_t achieved for this gel was 30−40 in the T_d range of 190−230 °C. Such dependences of the gel ductility on T_d and prior solution concentration indicate that the ductility of UHMW-PAN gel, with strong intermolecular interaction and fairly stiff chains, is also strongly controlled by the entanglement density, which likely increases with prior solution concentration. The effect of T_d on ductility of gels will be discussed below, based on the WAXD data.

It has been reported that the ductility of polymers increases above a crystalline α-relaxation[22] or a reversible crystal/crystal transition.[23,24] Two relaxations have been observed in PAN by dynamic mechanical tests: one occurring at 80−100 °C and the other at 140−160 °C, both at a frequency of 110 Hz. There have been controversies on the interpretation of these relaxations. Okajima et al.[25] have reported that the lower temperature relaxation is attributed to the molecular motion in the amorphous phase and the higher one to that in crystalline regions, based on the dynamic mechanical behavior of PAN fibers annealed under different conditions. In contrast, Minami et al.[26,27] attributed the lower relaxation to the molecular motion in paracrystalline regions and the higher one to that in amorphous regions, on the basis of the dynamic mechanical data on a series of PAN copolymers.

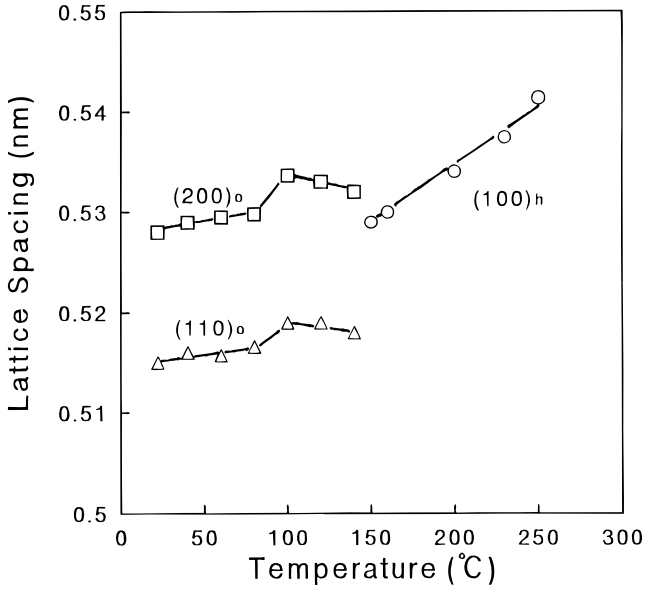

Figure 5. Temperature variations of the orthorhombic $(200)_o$ (□) and $(110)_o$ (△), and the hexagonal $(100)_h$ spacings (○) for a sample of a $DR_t = 30$.

The origins of the two mechanical relaxations have been studied by WAXD. PAN is one of the unusual polymers in that even an atactic sample can crystallize. There are controversies on the crystal structure of atactic PAN. As will be discussed later, however, we assume an orthorhombic unit cell with significant disorder along the chain axis, since one of the subjects to be discussed here concerns the changes of the two equatorial peaks around $2\theta = 17°$. Figure 5 shows the temperature variations of the orthorhombic $(200)_o$ and $(110)_o$ spacings. Both of the $(200)_o$ and $(110)_o$ spacings suddenly changed around 150 °C, and the two orthorhombic reflections merged into a single peak corresponding to the hexagonal $(100)_h$ reflection at $2\theta = 16.7°$. On cooling the sample, the hexagonal pattern reverted back to the orthorhombic pattern below 150 °C, indicating that this transition is reversible. Further, it is noted that the hexagonal $(100)_h$ spacing increases more rapidly with temperature than the orthorhombic $(200)_o$ and $(110)_o$ reflections, indicating a rapid chain separation above 150 °C, due to molecular motion activated in crystalline regions. These WAXD results show that the mechanical relaxation observed at 140−160 °C is related to the reversible crystal/crystal transition associated with molecular motion in the crystalline phase. Although the orthorhombic $(200)_o$ spacing in Figure 5 shows a notable change around 100 °C, such a change is not clear in the $(110)_o$ spacing vs temperature.

Thus, our X-ray data clearly show that the mechanical relaxation observed at 140−160 °C is due to the molecular motion in crystalline regions. However, there is no clear X-ray evidence that shows the relaxation at 80−100 °C ascribable to either phase. These results do indicate that the rapid increase in ductility above ∼150 °C may be ascribed to the gradual softening of crystals due to the onset of molecular motion in crystalline regions. A similar increase in ductility above the crystal relaxation temperature has been observed for other polymers.[13,17,22−24]

Structural Changes on Draw. There have been controversies on the crystal structure of PAN. Some authors[28−30] report a hexagonal chain packing with no order along the chain axis. Some other groups[10,31,32] propose an orthorhombic or pseudohexagonal cell with three-dimensional order. Recently, Bashir[30] extensively reviewed the crystal structure of PAN. He states that when PAN is treated with some solvents, the crystal becomes an orthorhombic cell having three-dimensional order. This is related to the cocrystallization of PAN with polar solvents, such as propylene carbonate, water, nitrobenzene, and others. Further, he observed that when such a solvated PAN was dried or highly elongated, the orthorhombic cell reverted to the hexagonal one with no periodicity along the chain direction. Thus, he concludes that the orthorhombic form of PAN is due to the solvation of PAN with small molecules.

The structural changes on draw of UHMW-PAN gel films have been studied by WAXD, SEM, and OM. Figure 6 shows WAXD patterns of a draw ratio series prepared from a 1 wt % gel film. The patterns taken with the incident X-ray beam both parallel and perpendicular to the film surface were identical. The WAXD of the original gel film in Figure 6a shows significantly strong diffuse scatterings from noncrystalline regions, in addition to the crystalline $(200)_o$, $(110)_o$, and (310, $020)_o$ reflection rings. These facts suggest that the crystallinity of the gel film is low and the crystallites are randomly oriented within the film. With increasing DR_t, the $(200)_o$, $(110)_o$, and $(310, 020)_o$ reflections became gradually sharper, and their azimuthal intensity distribution concentrated on the equator. Such changes in the WAXD pattern with DR_t indicate that the chains became progressively oriented and crystallized along the draw direction. Extremely high chain orientation and a high crystallinity were indicated by the circular reflection spots with no amorphous scatterings for a highly drawn sample of $DR_t = 106$ (Figure 6d). It is noted that the off-equatorial $(201)_o$ and $(002)_o$ reflections were observed in all the drawn samples, although the $(201)_o$ was broader than those of the equatorial ones. This, as well as the appearance of a streak on the second layer, suggests the existence of significant disorder along the chain axis.

To observe the $(002)_o$ reflection around $2\theta = 37°$ more clearly, WAXD photographs were recorded by tilting the samples to the incident beam by ∼18°. Figure 7 shows the WAXD tilt patterns of the extrudates with an EDR 6 and 16 and a highly drawn film of $DR_t = 80$. The scattering corresponding to the $(002)_o$, overlapped with a streak along the second layer line, was clearly observed on each of these patterns. Note that the crystal density (1.108 g/cm^3) calculated on the basis of a normal planar zigzag chain conformation with a repeat distance of 0.253 nm is significantly lower than the sample densities ranging 1.151−1.178 g/cm^3 (Figure 10). As the meridional scattering gives information on the conformation of PAN chains, diffractometer scans were made to examine the meridional scattering around $2\theta = 37°$ in more detail. The diffraction patterns of highly oriented fibers showed two peaks at $2\theta = 36.4°$ and 39.2°, which correspond to the spacings of 0.247 and 0.230 nm, respectively. According to the model calculations by Hu *et al.*,[33] these peaks correspond to the scatterings from syndiotactic (zigzag) and the isotactic (helical) sequences, respectively. This indicates that the average dimension of a monomer unit along the chain axis is significantly shorter than the normal planer zigzag conformation (0.253 nm). The crystal densities (1.135−1.220 g/cm^3), calculated assuming unit cell constants of $a = 1.03$ and $b = 0.61$ nm with $c = 0.247$ and 0.230 nm, and two chains penetrating a unit cell, are significantly higher than that (1.108 g/cm^3) calcu-

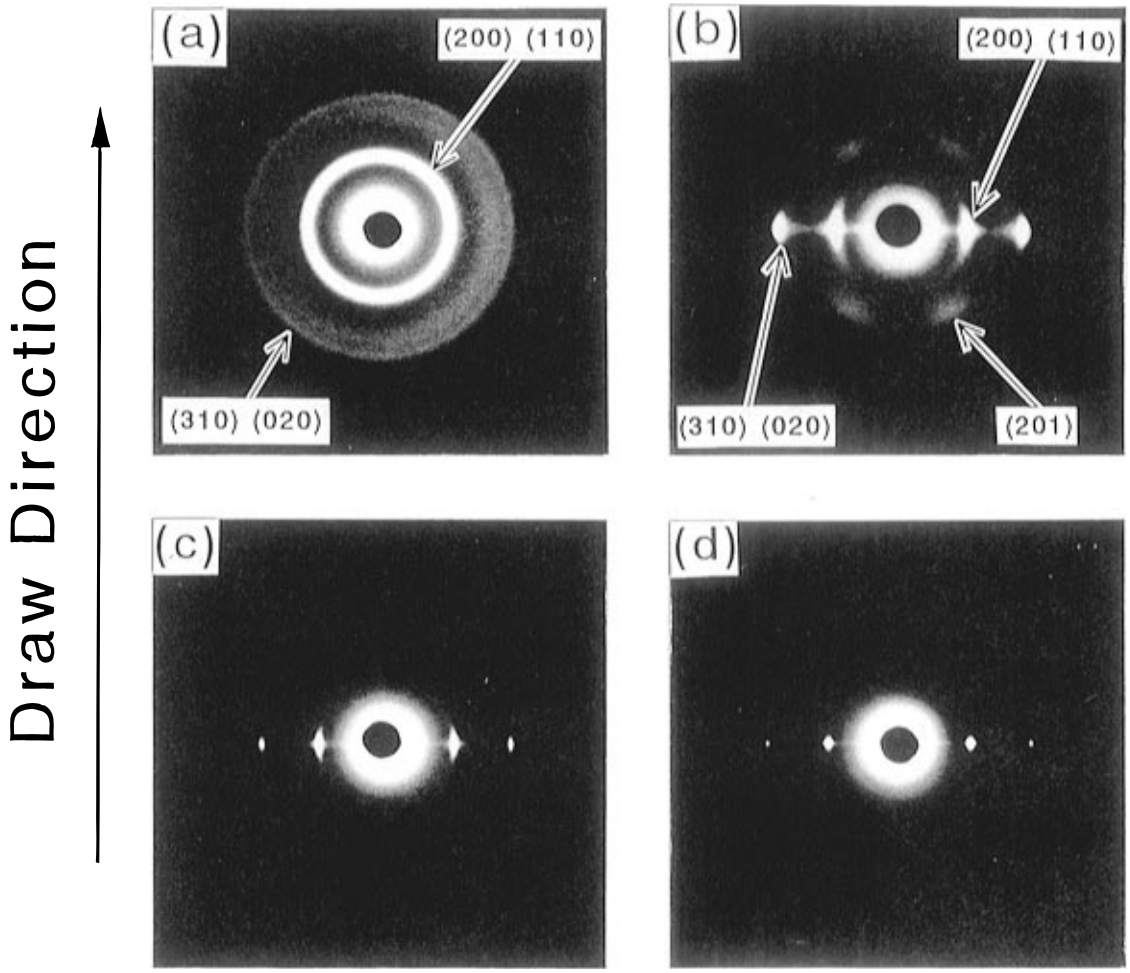

Figure 6. WAXD patterns for a series of drawn gel films: (a) initial 1 wt % gel; (b) EDR = 16; (c) $DR_t = 60$; (d) $DR_t = 106$.

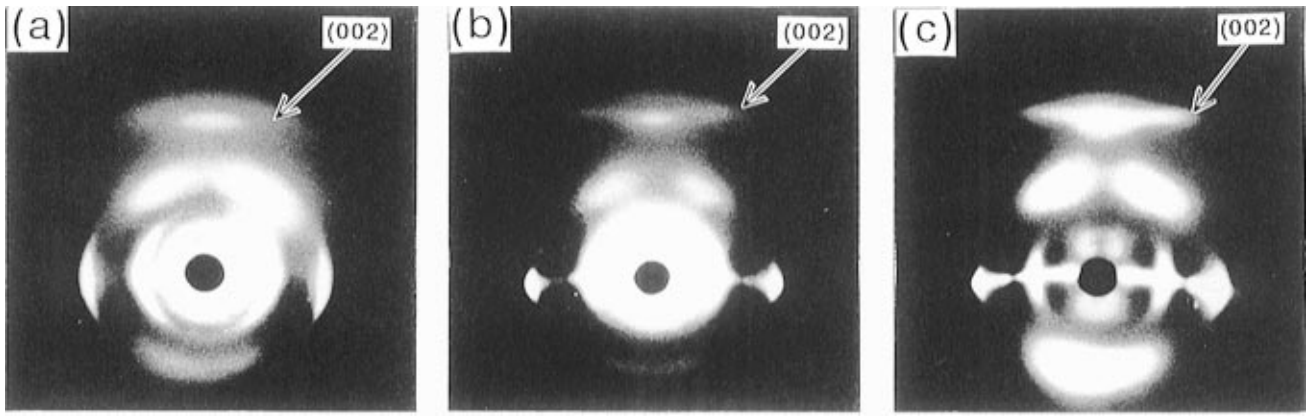

Figure 7. WAXD photographs for a series of drawn gel films, recorded by tilting the sample to the incident beam by ~18°: (a) EDR = 6; (b) EDR = 16; (c) $DR_t = 80$. Note that the orthorhombic $(002)_o$ reflection combined with a streak on the layer line is clearly seen.

lated assuming a planar zigzag chain conformation with a repeat distance of 0.253 nm. Thus, the observed fiber densities are consistent with the crystal densities estimated here. Further, Liu and Ruland[29] also discussed this problem in their two-dimensional Fourier transform analysis of the WAXD pattern of PAN fibers. They conclude that the conformation of PAN chains is predominantly planar zigzag with a finite persistence along the chain. They explained this persistence by the kinks related to the occurrence of isotactic sequences. They also showed that a small amount of such kinks (about one kink per ten monomer units), increases the theoretical crystal density up to a value consistent with the measured fiber densities.

We have also examined the polymorphism in PAN.[30] As seen in Figure 6, the WAXD photographs of a DR series show several reflections, such as the $(201)_o$ and $(002)_o$ reflections, which cannot be indexed on the basis of the hexagonal cell with no order along the chain direction. Especially, the equatorial reflection around $2\theta = 17°$ consists of double peaks, corresponding to the orthorhombic $(200)_o$ and $(110)_o$ reflections, as seen on the high-resolution diffractograms in Figure 8. The separation of the double peaks became more clear with increasing DR_t, indicating the development of crystalline order.

The overlapped reflections around $2\theta = 17°$ were decomposed into the $(200)_o$ and $(110)_o$ reflections, by

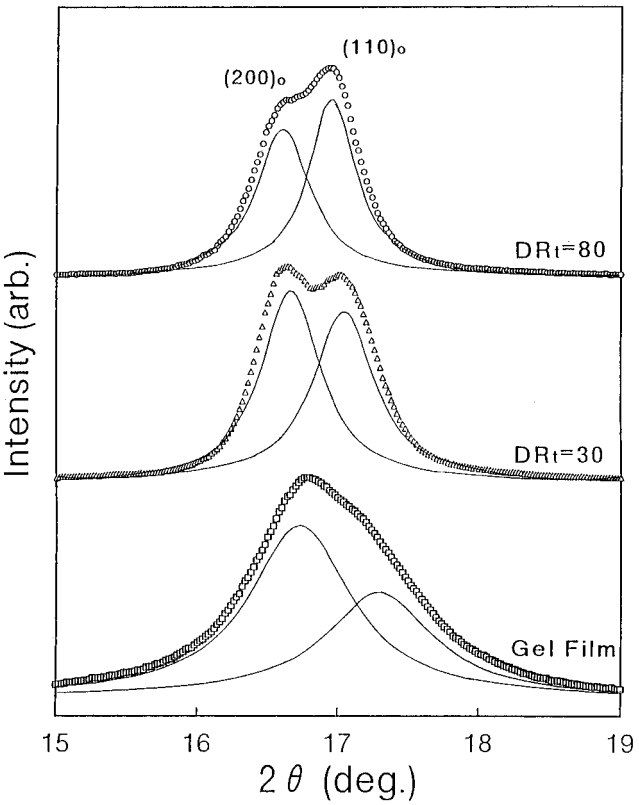

Figure 8. WAXD diffraction patterns for a draw ratio series, recorded at room temperature. The observed profiles were decomposed into the orthorhombic $(200)_o$ and $(110)_o$ reflections.

assuming a symmetrical function composed of Gaussian and Cauchy profiles, with appropriate portions for each of the reflections. The crystallite sizes, D_{200} and D_{110}, perpendicular to the chain axis were calculated from the decomposed reflection profiles, for drawing of a 1 wt % gel film. Both of the D_{200} and D_{110} increased rapidly with DR_t in the lower DR_t region, from the initial 8 nm to a constant of ~24 nm at higher $DR_t \geq 30$. These results also suggest that the regularity of chain packing improves with increasing DR_t.

The crystalline chain orientation was evaluated by the Herman orientation function f_c, determined by WAXD.[21] As the WAXD of PAN showed only the $(200)_o$ and $(110)_o$ reflections overlapped around $2\theta = 17°$ with a sufficient intensity, f_c was calculated from the azimuthal intensity distribution of this doublet, assuming fiber symmetry.[21] Figure 9 shows the crystalline chain orientation function f_c vs DR_t for two-stage draw of gel films at an optimum T_d. The f_c for each gel increased rapidly with DR_t in the lower range, and reached a $f_c > 0.98$ at an EDR = 16. At yet higher DR_t, it increased slowly with DR_t, reaching a maximum value of $f_c = 0.994-0.998$. These high f_c values indicate nearly perfect chain orientation of the highly drawn samples.

It should be mentioned here about our assumption that the azimuthal intensity distribution of the equatorial reflection is predominantly determined by the orientation distribution of the chain axes. This assumption may be critical for a highly oriented fiber with an f_c approaching unity. When the crystallite size is small and significant crystal disorder exists along the chain axis, the equatorial reflection is broadened perpendicular to the equator. The effects of such structural parameters on f_c may be qualitatively evaluated by the comparison of the f_c values calculated from reflections at low and high angles. The values obtained for a fiber

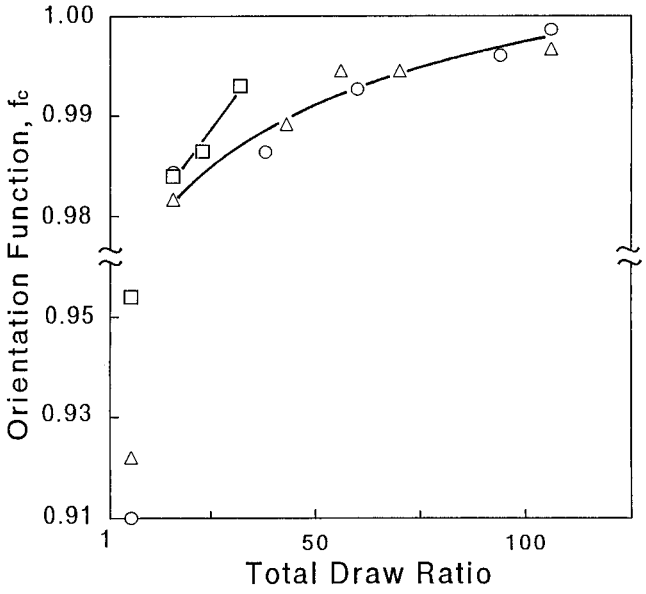

Figure 9. Crystalline chain orientation function f_c vs DR_t for two-stage draw of UHMW-PAN gel films prepared from different solution concentration: ○, 1 wt %; △, 2 wt %; □, 5 wt %.

of a DR_t 80 were $f_c = 0.993 \pm 0.002$ from the equatorial reflection around $2\theta = 30°$ and $f_c = 0.996 \pm 0.001$ from the strongest reflection around $2\theta = 17°$. The larger error for the former is related to the lower intensity of the reflection. The small difference between the two f_c values suggests that the azimuthal distribution of the equatorial reflection, and hence f_c, is predominantly determined by the orientation distribution of the chain axes, with a minor contribution from the reflection broadening due to the crystallite size and the crystal distortion along the chain axis.

For drawing of a gel film, prepared from a higher solution concentration of 5 wt %, f_c increased more rapidly with DR_t, although the highest achieved f_c (0.994) was slightly lower than that ($f_c = 0.998$) achieved for the gel film prepared from 1 wt % solution. This rapid increase in f_c for the 5 wt % gel film is ascribed to the higher entanglement density for the gel prepared from a solution of a higher concentration. The f_c values achieved in this work are significantly higher than the highest reported f_c of ~0.97 for PAN fibers and films.[12]

Figure 10 shows density vs DR_t for two-stage draw of gel films at the optimum T_d of 190 °C. Although the crystallinity could not be calculated from the sample density, as the amorphous density is not known for PAN, the observed density change with DR_t can be a measure of the structural change upon drawing. The density increased rapidly with DR_t from the initial $\rho = 1.151-1.154$ g/cm^3 for unoriented gel films to a limiting value of $1.172-1.179$ g/cm^3 at $DR_t \geq 25-30$, depending on gel. The gel film prepared from a higher solution concentration of 5 wt % showed a linear increase in density with DR_t, reaching a maximum of 1.179 g/cm^3 at the highest DR_t of 30. This is comparable to those of the highly drawn gels prepared from lower solution concentrations. Such an effect of prior solution concentration of a gel film on the increase in density with DR_t is similar to that observed in f_c vs DR_t. These results indicate that the structure of gel, prepared from a higher solution concentration, reorganizes more rapidly on draw due to the higher entangled state.

Figure 11 shows SEM (top) and OM (bottom) micrographs for a DR series prepared from a 1 wt % gel film.

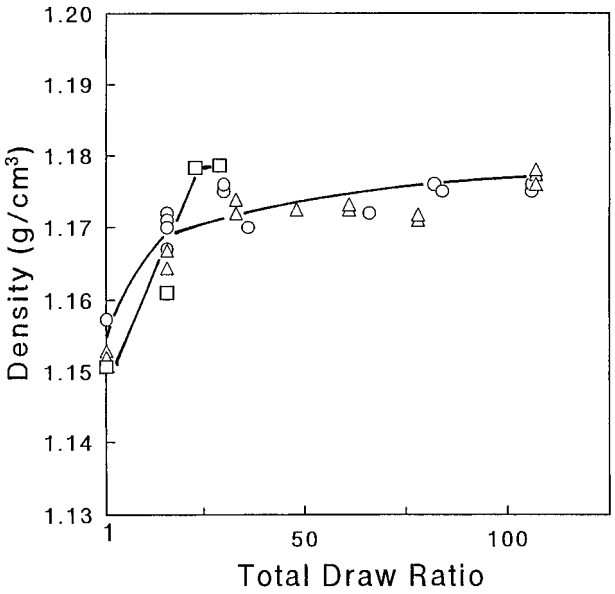

Figure 10. Density as a function of DR_t for draw of UHMW-PAN gel films prepared from 1 wt % (○), 2 wt % (△), and 5 wt % solution (□).

SEM micrographs reveal that the fibrils seen on the surface of an extrusion drawn sample with an EDR of 16 (Figure 11a) have not yet been well oriented along the draw direction. However, highly drawn samples (parts b and c of Figure 11) show well-developed fibrils running parallel to the draw direction, being consistent with the high chain orientation determined by WAXD (Figure 9). OM micrographs of an EDR = 16 extrudate and a drawn film of a DR_t 80 show a regular fibrous structure as observed by SEM. However, in an extremely drawn film with a DR_t = 106, a number of dark and bright lines are noted to run nearly perpendicular to the draw direction. As such heterogeneity was not revealed by the SEM observation of the surface, they likely exist within a drawn film. However, the chain orientation evaluated by f_c indicates nearly perfect chain orientation of the extremely drawn film, even if it exhibits such a heterogeneous optical feature. One possibility for such an optical property can be small thickness variations along the draw direction, even if the SEM did not reveal such surface roughness. This will be studied in the future.

Tensile Properties. Figure 12 shows tensile moduli vs DR_t for two-stage draw of UHMW-PAN gel films prepared from 1−5 wt % solutions. The second-stage draw was made on initially extrusion drawn samples with an EDR = 16 at an optimum T_d of 190 °C. The modulus of drawn gel films, prepared from lower solution concentrations of 1 and 2 wt %, increased rapidly with DR_t in the lower range and approached a constant value of 23−26 GPa at $DR_t \geq 75$. The constancy of modulus in the higher DR_t region and even its slight decrease at the highest DR_t of 106 are likely related to the formation of the optical heterogeneity observed by an OM (Figure 11c). The modulus for drawing of a gel film, prepared from a higher solution concentration of 5 wt %, increased more rapidly with DR_t than those prepared from lower solution concentrations. Although this sample exhibited low drawability, the maximum achieved modulus is close to that achieved for the highly drawable gel films prepared from lower solution concentrations. This is because the gel prepared from a higher solution concentration has a higher entanglement density, and therefore the chain orientation and extension proceeded more rapidly with DR_t, as shown in Figure 9. Actually, however, a slightly higher modulus was achieved for the gel prepared from a lower solution concentration (26 vs 23 GPa). The maximum achieved modulus of 26 GPa is 2.5−3.5 times higher than that (7−10 GPa) of commercial PAN fibers[34] and approaches the uncertain X-ray crystal modulus of atactic PAN (28 GPa[11]).

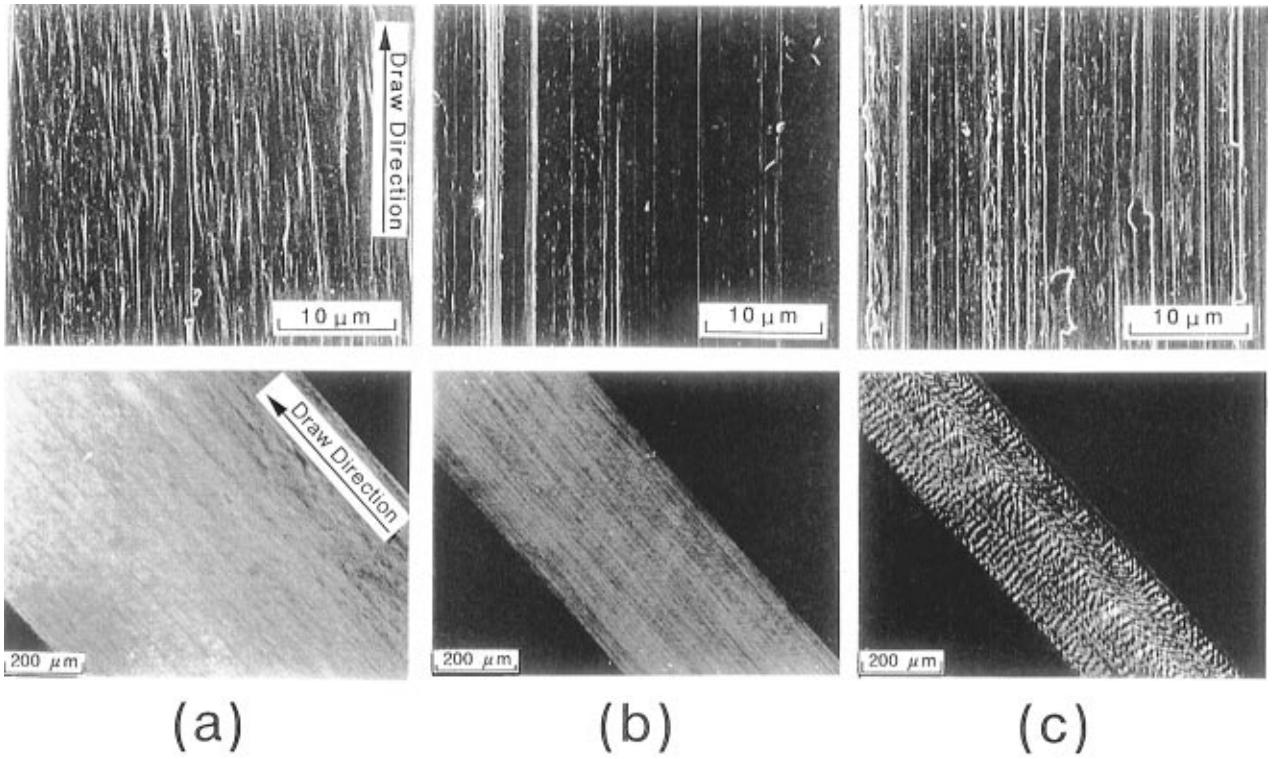

Figure 11. SEM (top) and OM (bottom) micrographs for a series of drawn gel films: (a) EDR = 16; (b) DR_t = 78; (c) DR_t = 106 film. The OM observations were made under crossed polarizers. Samples were oriented at an angle of 45° to the polarizers.

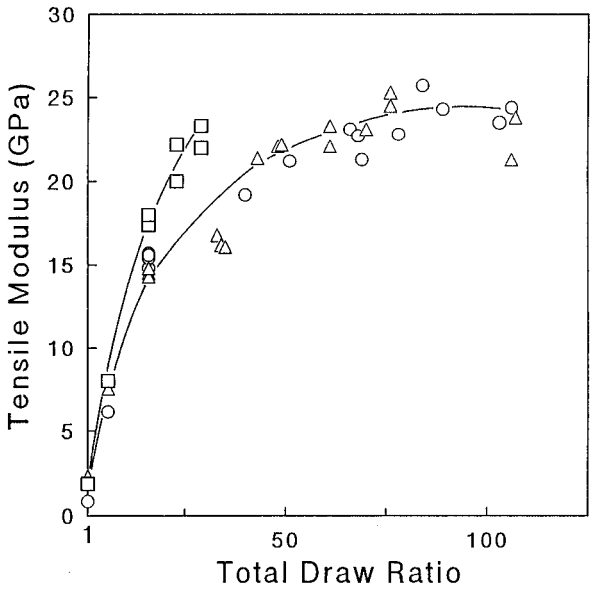

Figure 12. Tensile modulus as a function of DR_t for two-stage draw of UHMW-PAN gel films prepared from different solution concentrations: ○, 1 wt %; △, 2 wt %; □, 5 wt %.

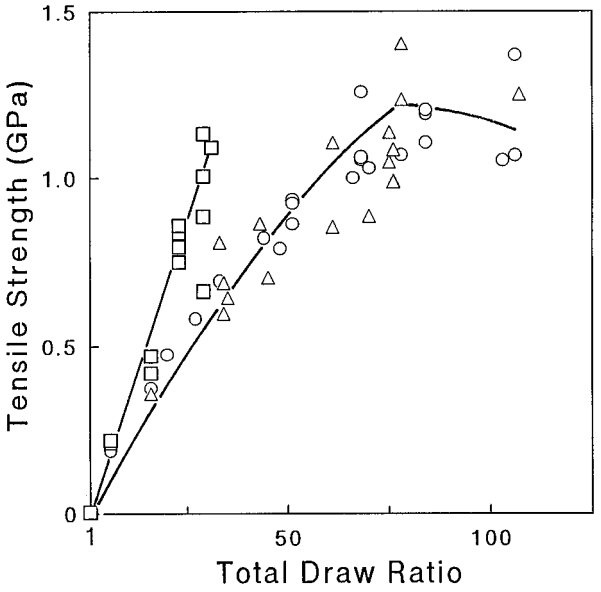

Figure 13. Tensile strength as a function of DR_t for two-stage draw of UHMW-PAN gel films prepared from different solution concentrations: ○, 1 wt %; △, 2 wt %; □, 5 wt %.

Figure 13 shows tensile strength vs DR_t for two-stage draw of UHMW-PAN gel films. The second-stage draw was made at an optimum T_d for each of them (Figure 4). The strength of drawn gels, prepared from lower solution concentrations of 1 and 2 wt %, increased linearly with DR_t in the lower region, reaching a maximum value of 1.1−1.4 GPa at $DR_t \geq 85$. At the highest DR_t of 106, the strength also decreased slightly. Such a decrease in the strength at the highest DR_t can also be related to the formation of the optical heterogeneity observed by an OM (Figure 11c), as was discussed in the tensile modulus vs DR_t. The strength of 5 wt % gel increased more rapidly with DR_t in the lower region and reached a maximum of 0.85−1.1 GPa at the highest achieved DR_t of 30.

The strain at break was in the range of 7−8% for highly drawn gel films, independent of prior solution concentration for gelation. These results show that slightly higher modulus and strength were achieved by two-stage drawing of UHMW-PAN gel films prepared from a lower solution concentration of 1−2 wt % than those achieved for the gel from a higher solution concentration of 5 wt %.

Conclusions

Dry gel films of UHMW-PAN prepared from 1−5 wt % solutions have been ultradrawn by a two-stage draw technique, consisting of the first-stage solid-state coextrusion at a low EDR of 8−16, followed by the second-stage tensile draw at 100−235 °C. Drawability of gels and uniformity of the resultant drawn products were strongly affected by the prior solution concentration, initial EDR, and second-stage draw temperature. The $DR_{t,max}$ of a gel film increased with decreasing prior solution concentration, suggesting that the ductility of UHMW-PAN, with fairly strong intermolecular interaction and high chain stiffness, is also affected by the chain entanglement density. The drawability of gels prepared from lower solution concentrations of 1 and 2 wt % increased rapidly with T_d above ~150 °C, reaching a maximum at 190 °C, and then decreased sharply at yet higher temperatures. This rapid increase in ductility above 150 °C, as well as the high ductility of gel, is ascribed to the crystal softening due to the onset of molecular motion above the reversible crystal/crystal transition at 150 °C, which was detected by the WAXD. The highest uniform DR_t of 110 was achieved by the first-stage coextrusion draw of a 1 wt % gel film to an EDR of 16, followed by the second-stage tensile draw at 190 °C. The highly drawn samples showed extremely high chain orientation of $f_c = 0.998$. Thus, the highest tensile modulus of 26 GPa and strength of 1.3 GPa were achieved by two-stage draw of the gel films prepared from a low solution concentration of 1−2 wt %. These values are slightly higher than those achieved by solid-state coextrusion alone[8] and comparable to the highest values reported for UHMW-PAN fibers.[12] Further, the highest achieved modulus is close to the uncertain X-ray crystal modulus of atactic PAN (28 GPa).[11] The temperature variations of WAXD patterns of drawn films showed that the PAN crystal takes on an orthorhombic chain packing at lower temperatures, independent of draw temperature and DR_t. It transforms into the hexagonal packing above 150 °C, where the chain motion is activated in the crystal. This change in the crystal structure with temperature is reversible.

References and Notes

(1) Smook, J.; Vos, G. J. H.; Doppert, H. L. *J. Appl. Polym. Sci.* **1990**, *41*, 105.
(2) Kunugi, T.; Akiyama, I.; Hashimoto, M. *Polymer* **1982**, *23*, 1193.
(3) Gogolewski, S.; Pennings, A. J. *Polymer* **1985**, *26*, 1394.
(4) Kunugi, T.; Ichinose, C.; Suzuki, A. *J. Polym. Sci., Polym. Phys. Ed.* **1990**, *25*, 2127.
(5) Huang, B.; Ito, M.; Kanamoto, T. *Polymer* **1993**, *35*, 1210.
(6) Walker, E. E. *J. Appl. Chem.* **1952**, *2*, 470.
(7) Krigbaum, W. R.; Tokita, N. *J. Polym. Sci.* **1960**, *43*, 647.
(8) Kameda, T.; Kanamoto, T. *J. Soc. Rheol. Jpn.* **1993**, *21*, 156.
(9) Kameda, T.; Yamane, A.; Kanamoto, T.; Ito, M.; Porter, R. S. *Vysokomol. Soed. Ser. A* **1996**, *38*, 1152.
(10) Kumamaru, F.; Kajiyama, T.; Takayanagi, M. *J. Cryst. Growth* **1980**, *48*, 202.
(11) Allen, R. A.; Ward, I. M.; Bashir, Z. *Polymer* **1994**, *35*, 4035.
(12) Dobretsov, S. L.; Lomonosova, N. V.; Stelmakh, V. P.; Frenkel, S. Ya. *Vysokomol. Soed.* **1972**, *A14*, 1143 (English Translation). The authors of this paper evaluated the chain orientation by the half-width of azimuthal intensity distribution ($\Delta\psi$) of the reflection at $2\theta = 17°$. Thus, the highest f_c value of 0.97 was estimated from the smallest reported value of

$\Delta\psi = 8° 24'$, assuming the same azimuthal intensity distribution function as observed in this work.
(13) Kanamoto, T.; Tsuruta, A.; Tanaka, T.; Takeda, M.; Porter, R. S. *Macromolecules* **1988**, *21*, 470.
(14) Kanamoto, T.; Porter, R. S. In *Integration of Fundamental Polymer Science and Technology*; Lemstra, P. J., Kleintjens, L. A., Eds.; Elsevier Appl. Sci.: London, 1989; Vol. 3, p 168.
(15) Kanamoto, T.; Ohtsu, O. *Polym. J.* **1988**, *20*, 179.
(16) Kanamoto, T.; Ohama, T.; Tanaka, K.; Takeda, M.; Porter, R. S. *Polymer* **1987**, *28*, 1517.
(17) Uehara, H.; Jounai, K.; Endou, R.; Okuyama, H.; Kanamoto, T.; Porter, R. S. *Polym. J.* **1997**, *29*, 198.
(18) Griswold, P. D.; Zachariades, A. E.; Porter, R. S. *Polym. Eng. Sci.* **1978**, *18*, 861.
(19) Kobashi, T.; Takagi, A. Tokkyo-Koukai (A), Syowa 60-139810 (Japan).
(20) Brandrup, J.; Immergut, E. H. *Polymer Handbook*; John Wiley & Sons: New York, London, Sydney, Tronto, 1974.
(21) Alexander, L. E. *X-ray Diffraction Methods in Polymer Science*; John Wiley & Sons: New York, 1969.
(22) Takayanagi, M. *Koubunshi (High Poymer, Jpn.)* **1966**, *10*, 289.
(23) Aharoni, S. M.; Sibilia, J. P. *J. Appl. Polym. Sci.* **1979**, *23*, 133.
(24) Saraf, R.; Porter, R. S. *J. Polym. Sci., Polym. Phys. Ed.* **1988**, *26*, 1049.
(25) Okajima, S.; Ikeda, M.; Takeuchi, A. *J. Polym. Sci., A-1* **1968**, *6*, 1925.
(26) Minami, S.; Yoshihara, T.; Sato, H. *Koubunshi Kagaku* **1972**, *29*, 109.
(27) Minami, S.; Yoshihara, T.; Sato, H. *Koubunshi Kagaku* **1972**, *29*, 114.
(28) Bohn, C. R.; Schaefgen, J. R.; Statton, W. O. *J. Polym. Sci.* **1961**, *55*, 531.
(29) Liu, X. D.; Ruland, W. *Macromolecules* **1993**, *23*, 3030.
(30) Bashir, Z. *J. Polym. Sci., Polym. Phys. Ed.* **1994**, *32*, 1115.
(31) Holland, V. F.; Mitchell, S. B.; Hunter, W. L.; Lindenmeyer, P. H. *J. Polym. Sci.* **1962**, *62*, 145.
(32) Hinrichsen, G.; Orth, H. *Kolloid-Z. Polym.* **1971**, *247*, 844.
(33) Hu, X.; Johnson, D. J.; Tomka, J. G. *J. Text. Inst.* **1995**, *86*, 322.
(34) Oota, T.; Kunugi, T.; Yabuki, K. *High Strength and High Modulus Fibers*; Kyouritsu: Tokyo, 1988.

MA9614095